ENVIRONMENTAL RESEARCH
COMMUNICATIONS

INCLUSIVE PUBLISHING TRUSTED SCIENCE

Part of the ENVIRONMENTAL RESEARCH SERIES

PURPOSE-LED PUBLISHING™

LETTER • OPEN ACCESS

Future wildfire risk to population and property in the contiguous US: a scenario-based assessment

To cite this article: Jianyong Ma *et al* 2026 *Environ. Res. Commun.* **8** 111003

View the article online for updates and enhancements.

You may also like

- Social vulnerability of Pandeglang Regency, Banten
D A Lestari, N S Fitriasari, D R Azhari et al.
- Wireless communication network security intelligent monitoring system based on machine learning
Hongkun Liu, Nianci Wang and Sirong Liang
- Groundwater Vulnerability Zones Mapping Using DRASTIC and GOD Methods in Krendowahono Village, Karanganyar Regency
Sorja Koesuma, Umi Rosidah and Ari Handono Ramelan

SmarAct | group

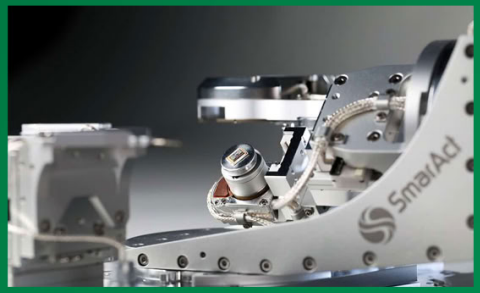
webinar

More details and registration

One sample, many dimensions: prospects for multimodal nanoscale characterization

Explore how precise sample manipulation enables complementary nanoscale techniques to work together on one sample

Live at 2 p.m. GMT/3 p.m. CET,
12 November 2026



This content was downloaded from IP address 129.13.194.163 on 16/11/2026 at 09:33

Environmental Research Communications

Check for updates

OPEN ACCESS

RECEIVED
23 September 2026

REVISED
6 October 2026

ACCEPTED FOR PUBLICATION
28 October 2026

PUBLISHED
4 November 2026

Original content from this work may be used under the terms of the Creative Commons Attribution 4.0 licence.

Any further distribution of this work must maintain attribution to the author(s) and the title of the work, journal citation and DOI.

LETTER

Future wildfire risk to population and property in the contiguous US: a scenario-based assessment

Jianyong Ma[1,*], **Ashton Dickinson**[1,2], **Anja Rammig**[2], **Martin Wittenbrink**[1] and **Almut Arneth**[1,3]

[1] IMK-IFU, Global Land-Ecosystem Modelling Group, Karlsruhe Institute of Technology, Garmisch-Partenkirchen, Germany
[2] School of Life Sciences, Technical University of Munich, Freising, Germany
[3] Institute of Geography and Geoecology, Karlsruhe Institute of Technology, Karlsruhe, Germany
[*] Author to whom any correspondence should be addressed.

E-mail: jianyong.ma@kit.edu

Keywords: wildfire burned area, social vulnerability index, wildland-urban interface, risk assessment

Supplementary material for this article is available online

Abstract

Despite growing concern about wildfire impacts on human societies under climate and socioeconomic change, existing studies often examine individual drivers or focus on regional patterns, limiting our understanding of how wildfire risk may vary across communities at the national scale. Here, we develop a county-level framework that integrates wildfire hazard, exposure, and community vulnerability to assess future wildfire risk across the contiguous United States (CONUS). Using projections of annual burned area, population and property distributions, wildland-urban interface (WUI) extent, and a social vulnerability index under three shared socioeconomic pathways (SSPs), we assess changes in population and property wildfire risk through the end of the 21st century. Our results show that the western forested and Rocky Mountain regions currently face the highest wildfire risk resulting from high burn probabilities, elevated social vulnerability, and extensive WUI areas, whereas most counties in the northern Great Plains experience relatively low risk because of limited fire activity, lower social vulnerability, and sparse WUI. Future projections indicate substantial spatial heterogeneity in risk changes: many areas with currently high risk remain among the highest-risk regions, while some historically low-risk counties transition toward higher risk, driven primarily by increases in population exposure and social vulnerability. By the end of the century, population and property risks across the CONUS are projected to rise by 54%–411% and 19%–160%, respectively, under three SSP scenarios. These findings highlight the need to extend wildfire management strategies beyond currently high-risk areas to account for emerging shifts in wildfire risk across the CONUS.

1. Introduction

Many regions globally have experienced extraordinarily large wildfires in recent years, with several events characterized by exceptional intensity and prolonged duration (Bowman *et al* 2017, Turco *et al* 2023, Cunningham *et al* 2024, Seydi *et al* 2025). Large and intense wildfires pose serious threats to both people and property, with the contiguous United States (CONUS) emerging as a prominent hotspot (Radeloff *et al* 2018, Rad *et al* 2023b, Liu *et al* 2025). Over the past two decades, the population and housing within fire-affected areas of the CONUS have grown by 125% and 36%, respectively (Radeloff *et al* 2023, Rad *et al* 2023b). This trend reflects a substantial expansion in wildfire burned area (BA), which has roughly increased by sevenfold in the United States between 1983 (∼5400 km^2) and 2024 (∼36000 km^2; National Interagency Fire Center 2024). Given that wildfire activity is expected to persist at current levels or likely intensify in many regions due to ongoing climate change and shifts in population distribution and vegetation dynamics (Ager *et al* 2021, Ellis *et al* 2022, Pomara *et al* 2025), there is a clear need to improve assessment of future wildfire risks to human communities and infrastructure, in order to mitigate the potential loss of life and property.

© 2026 The Author(s). Published by IOP Publishing Ltd

A widely adopted framework for risk assessment involves integrating information across multiple dimensions, including hazard, exposure, and vulnerability (IPCC AR6; see Begum *et al* 2022). Hazard typically refers to the probability and intensity of wildfire occurrence; exposure describes the extent to which a potential fire overlaps with elements that may be affected; and vulnerability reflects the susceptibility of those exposed to harm (Zuzak *et al* 2022, Chuvieco *et al* 2023). Within this framework, the exposure includes both human populations and physical assets. These are closely related, but they may be associated with different vulnerability factors and impact pathways. This is why we treat them separately in our analysis.

For human populations, social vulnerability—defined as the demographic and socioeconomic factors that influence a community's ability to prepare for and respond to hazards (Cutter *et al* 2003, Flanagan *et al* 2011)—is increasingly incorporated into wildfire risk assessment to characterize differences in the susceptibility of exposed communities (Lambrou *et al* 2023). For instance, Rad *et al* (2023a) found that in California, increases in social vulnerability within BAs were the main driver of rising population exposure, whereas in Oregon and Washington, the expansion of BAs into socially vulnerable communities played a more important role. Being closely related to social vulnerability for residential properties, the wildland-urban interface (WUI)—areas where wildland vegetation and residential development meet or intermingle (Radeloff *et al* 2005, 2018)—provides a more direct representation of the physical conditions associated with wildfire impacts on residential structures. WUI areas account for a disproportionate share of housing loss during wildfire events in the United States (National Interagency Fire Center 2024). Between 1990 and 2020, the WUI in the CONUS is estimated to have expanded by 34% in total land area and by 43% in terms of number of houses (Radeloff *et al* 2023), reflecting growing spatial overlap between human settlements and fire-prone landscapes. Yet despite of these rapid dynamics, most existing risk assessments remain confined to historical or present-day conditions (e.g. Zuzak *et al* 2022, Nepal *et al* 2023), largely due to a lack of temporally and spatially explicit projections of future social vulnerability and WUI development—despite recent availability of wildfire BA projections from both data-driven (Zhang *et al* 2024) and process-based models (Wu *et al* 2021, Li *et al* 2024).

To respond to the need for future-oriented assessments, this study builds on the integrative framework proposed by Begum *et al* (2022) and introduces a spatially explicit, forward-looking approach for evaluating wildfire risk across the United States. Specifically, we integrate projections of wildfire BA, population demographics, and dynamic estimates of social vulnerability and WUI extent under different future climate pathways (figure 1). Our objective is to identify where wildfire risk to populations and properties may intensify at the county level in the coming decades, relative to the historical baseline. The findings are intended to offer opportunities to support homeowners, developers, and public agencies in making land-use decisions that minimize exposure to future wildfire hazard.

2. Data and method

This study uses shared socioeconomic pathways (SSPs; e.g. O'Neill *et al* 2014) to represent future socioeconomic conditions and evaluate their implications for wildfire risk. To capture a range of plausible socioeconomic trajectories, we focus on SSP1, SSP3, and SSP5 scenarios, representing sustainable development, regional rivalry, and fossil-fueled expansion, respectively (Riahi *et al* 2017; also see Text S1 in the supplementary information for a more detailed description of each SSP scenario). To contrast mid- and long-term changes, we analyze future projections for two periods—2041–2050 and 2091–2100—relative to historical baseline of 2005–2014. Details of the data sources and methods used to quantify wildfire hazard, population and property exposure, social vulnerability, and WUI areas under the three SSP scenarios are described in the following sections (see also table 1).

2.1. Wildfire BA

We use gridded annual BA outputs from process-based wildfire models participating in the Inter-Sectoral Impact Model Intercomparison Project (ISIMIP3a and 3b) to characterize the fire hazard for both historical and future periods. Comparing with present-day analyses based on satellite-derived BA (e.g. Seydi *et al* 2025), this approach enables seamless projection of BA into future. Based on recent evaluation by Liu *et al* (2025), the ELM model outperforms the other seven ISIMIP participants in capturing the spatial pattern and magnitude of BA across the CONUS during 2001–2019. We therefore adopt the ensemble mean of ELM outputs, driven by five general circulation models, as the hazard input for our wildfire risk assessment (ISIMIP Repository 2025). To match county-level population demographic statistics (see section 2.2), the original 0.5° resolution BA outputs are aggregated to the county scale using area-weighted averaging of grid cells intersecting each county boundary (see Text S1 in the supplementary

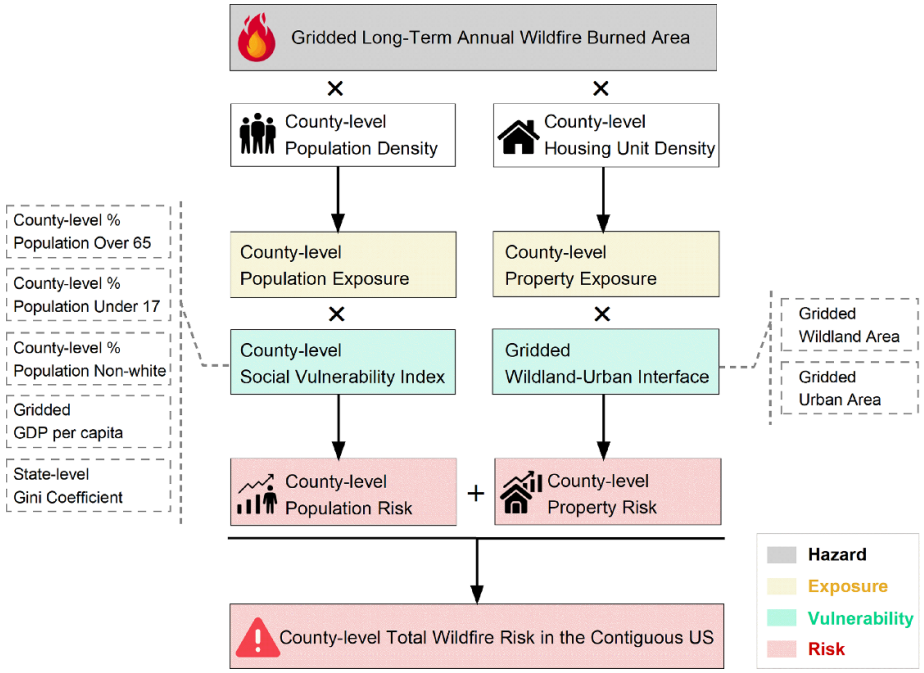


Figure 1. Flowchart of the wildfire risk assessment framework applied in this study, illustrating the integration of hazard, exposure (population and property), and vulnerability components under historical and future SSP scenarios.

information for details of future BA projections from the ELM model). Based on these county-level BA estimates, the population and property exposure to wildfire are calculated as:

$$\text{Exposure}_i = \text{BA}_i \times \text{Density}_i \tag{1}$$

where BA_i is the estimated total BA (km^2; figure S1 in the supplementary information) in county i, and Density_i denotes either population density (people/km^2; figure S2 in the supplementary information) or housing unit density (buildings/km^2; figure S3 in the supplementary information) for that county. A total of 3109 counties across the CONUS are included in the analysis.

2.2. Social vulnerability index (SoVI)

There is no universally adopted definition of social vulnerability, nor a standardized set of indicators commonly used in natural hazard assessments (Davies *et al* 2018, Flanagan *et al* 2018). This challenge is particularly pronounced in forward-looking studies, where the selection of indicators is constrained by the limited availability of relevant data consistent with the SSP framework (e.g. KC *et al* 2021, Landreau *et al* 2021). In this study, we use five indicators—population aged over 65, population under 17, non-white population (race/ethnicity), GDP per capita (income), and the Gini coefficient (poverty inequality)—to broadly construct the county-level SoVI. These indicators, reviewed by Lambrou *et al* (2023), are used in the wildfire vulnerability literature (e.g. Wigtil *et al* 2016, Federal Emergency Management Agency [FEMA] 2025) and can be projected under SSP-based socioeconomic scenarios. The data sources for the historical and future values of these five indicators are summarized in table 1.

To address unit inconsistencies among the five indicators, each variable is normalized to a 0–1 scale using percentile ranks computed across all 3109 counties and all time periods combined, following the approach of Flanagan *et al* (2011). The overall SoVI for each county is then obtained by summing the five normalized indicators with equal weight (equation (2). This two-step method captures each county's relative position within the national distribution over time, with higher values reflecting greater vulnerability,

$$\text{SoVI}_i = [\text{PR}(\%\text{Over65}_i) + \text{PR}(\%\text{Under17}_i) + \text{PR}(\%\text{Nonwhite}_i) + \text{PR}\left(\frac{1}{\text{GDP}_i}\right) + \text{PR}(\text{Gini}_i)]/5 \tag{2}$$

where PR denotes the percentile ranking normalization method; $\%\text{Over65}_i$, $\%\text{Under17}_i$, and $\%\text{Nonwhite}_i$ represent the proportions of population aged over 65, under 17, and non-white, respectively, in county i. GDP_i refers to GDP per capita (PPP 2005 US dollars). Because higher GDP per capita generally indicates

Table 1. Summary of input data used in this study, categorized by type, spatial scale, and temporal coverage. Future data are available for the SSP1, SSP3, and SSP5 scenarios.

Variable	Description	Data type	Spatial scale	Temporal scale	Source
Annual burned area from wildfires (km^2)	Derived from the ELM model outputs of ISIMIP3a and ISIMIP3b simulations, and used as the basis for computing population and property exposure.	Historical; 3 SSPs	0.5° raster[a]	1850–2014; 2015–2100	ISIMIP Repository (2025)
Population density (people/km^2)	Employed to compute historical population exposure in conjunction with burned area.	Historical	County level	2010	CDC/ATSDR (2010)
Population density (people/km^2)	Employed to compute future population exposure in conjunction with burned area.	3 SSPs	County level	2020–2100	Hauer (2019)
Housing unit density (buildings/km^2)	Employed to compute property exposure in conjunction with burned area.	Historical 3 SSPs[b]	County level	2010	CDC/ATSDR (2010)
(i) Population aged 65 and older (%) (ii) Population aged 17 and younger (%) (iii) Non-white population (%)	Employed to compute the historical social vulnerability index (SoVI) in conjunction with GDP per capita and the Gini coefficient. The SoVI is then used to calculate population risk.	Historical	County level	2010	CDC/ATSDR (2010)
(i) Population aged 65 and older (%) (ii) Population aged 17 and younger (%) (iii) Non-white population (%)	Employed to compute the future SoVI in conjunction with GDP per capita and the Gini coefficient.	3 SSPs	County level	2020–2100	Hauer (2019)
GDP per capita (PPP 2005 US dollars)	Employed to compute the SoVI in conjunction with population demographics and the Gini coefficient.	Historical; 3 SSPs	1 km raster[a]	2000–2020; 2025–2100	Wang and Sun (2022)
Gini coefficient (unitless; 0–1)	Employed to compute the SoVI in conjunction with population demographics and GDP per capita.	Historical; 3 SSPs	State level[c]	2010–2015; 2020–2100	Casper *et al* (2023)
Wildland area (%)	Used to compute the wildland-urban interface (WUI) in conjunction with urban area fraction. The WUI is then used to calculate property risk.	Historical; 3 SSPs	1 km raster[a]	2015; 2020–2100	Chen *et al* (2022)
Urban area (%)	Used to compute the WUI in conjunction with wildland area fraction.	Historical; 3 SSPs	1 km raster[a]	2015; 2020–2100	Chen *et al* (2022)

[a] Raster data are aggregated to the county level for the contiguous US.
[b] In the absence of future housing unit data, historical values from 2010 are used for all three SSP scenarios.
[c] State-level data are used to represent the corresponding counties.

greater economic capacity and lower social vulnerability, its inverse ($1/GDP_i$) was used before normalization to ensure that all five indicators have the same direction, with higher values representing greater social vulnerability. $Gini_i$ is the Gini coefficient ranging from 0–1. Changes in these five indicators for the historical and future periods under three SSP scenarios are visualized in figure S4 (supplementary information), with the resulting SoVI for the same periods presented in figure S5 (supplementary information).

2.3. WUI

The US Federal Register defines two types of the WUI: intermix and interface (Radeloff *et al* 2005). Intermix WUI describes areas with a housing density above 6.17 buildings/km^2 and over 50% wildland vegetation. Interface WUI, by contrast, refers to areas with similar housing density but less than 50% vegetation cover, located within 2.4 km of a large adjacent patch (>5 km^2 with $\geqslant$ 75% wildland vegetation).

Identifying WUI areas typically requires high-resolution information on vegetation cover and residential development, such as building footprints (Carlson *et al* 2022), structure locations (Bar-massada *et al* 2013), or housing datasets (e.g. Schug *et al* 2023, Chen *et al* 2024). However, such detailed information is usually unavailable for future SSP-based projections. Schug *et al* (2023) identified candidate WUI pixels using building-density-based criteria, with >0.5% aggregated building density indicating potential WUI and >15% indicating urban characteristics. Here, we approximate future WUI dynamics using 1 km gridded land-use data from Chen *et al* (2022). Grid cells with >50% a wildland fraction and 0.5%-15% urban land fraction are classified as WUI, representing mixed wildland-human landscapes. This land-cover-based approach is intended as a proxy for future WUI patterns rather than a direct conversion of building-density thresholds used by Schug *et al* (2023). County-level WUI extent is then calculated as the area-weighted sum of WUI grid cells intersecting each county (see Text S1 in the supplementary information for details of land-use processing and WUI derivation):

$$\mathrm{WUI}_i = \sum_{j=1}^{n} \mathrm{WUI}_{i,j} \; \forall(\mathrm{Wildland}_{i,j} > 50\%) \;\&\; (0.5\% \leqslant \mathrm{Urban}_{i,j} \leqslant 15\%) \tag{3}$$

where $\mathrm{Wildland}_{i,j}$ and $\mathrm{Urban}_{i,j}$ represent the fractions of wildland vegetation and urban land, respectively, for grid cell j within county i; WUI_i is the total WUI area of county i, expressed in km^2. Estimates of total wildland and urban areas across the CONUS for historical and future periods under three SSP scenarios, along with visualizations of county-level WUI patterns, are presented in figures S6 and S7 in the supplementary information.

2.4. Total risk score and level

Following the National Risk Index methodology developed by the US Federal Emergency Management Agency (Federal Emergency Management Agency [FEMA] 2025), county-level population and property risk scores are first standardized independently and then summed to compute total risk scores:

$$\begin{cases} \text{Population Risk Score}_i = \text{Exposure}_{\text{POP}i} \times \text{PR}(\text{SoVI}_i) \\ \text{Property Risk Score}_i = \text{Exposure}_{\text{PRO}i} \times \text{PR}(\text{WUI}_i) \\ \text{Total Risk Score}_i = \text{PR}(\text{Population Risk Score}_i) + \text{PR}(\text{Property Risk Score}_i) \end{cases} \tag{4}$$

where $\text{Exposure}_{\text{POP}i}$ and $\text{Exposure}_{\text{PRO}i}$ are the population and property exposure, respectively, as calculated from equation (1). Estimates of SoVI_i and WUI_i for county i are taken from equations (2) and (3) and rescaled to a 0–1 range using percentile ranks across all CONUS counties and time periods. The resulting total risk scores (ranging from 0–2) are further categorized into five levels—Very Low, Low, Moderate, High, and Very High—using national quintile-based thresholds (20% intervals) derived from the historical baseline period. The specific cutoff values for each risk category are listed in table S1 in the supplementary information.

3. Results

3.1. Historical exposure, vulnerability, and wildfire risk

The maps of population exposure to wildfires from our study align well with those from the US Federal Emergency Management Agency (Federal Emergency Management Agency [FEMA] 2025), with a spatial correlation coefficient of 0.57 ($p < 0.001$), although our estimates tend to be higher in some southeastern counties (figure 2(a)). Both analysis identify exposure hotspots in the western and southern CONUS, driven by high wildfire probability and population density (figures S1 and S2 in the supplementary information). In contrast, much of the northern Great Plains—such as eastern Montana, the Dakotas, Nebraska, and Iowa—shows low exposure. Similar spatial patterns emerge for property exposure; however, FEMA's results display greater variability in the relationship between population and property exposure than our study (figure S3 in the supplementary information), primarily because FEMA further adjusts its estimates using county-level historical loss ratios.

Our findings are spatially consistent with the SoVI developed by the US Centers for Disease Control and Prevention (CDC/ATSDR 2010), showing a high correlation coefficient of 0.91 ($p < 0.001$). In this study, the highest social vulnerability occurs along the West Coast and much of the southern CONUS (figure 2(b)), due to a higher proportion of non-white populations and residents under age 17, as well as relatively low per capita GDP in the Southeast. Likewise, high WUI areas—reflecting property vulnerability to wildfires—are estimated in the western forested mountains and the temperate forests of

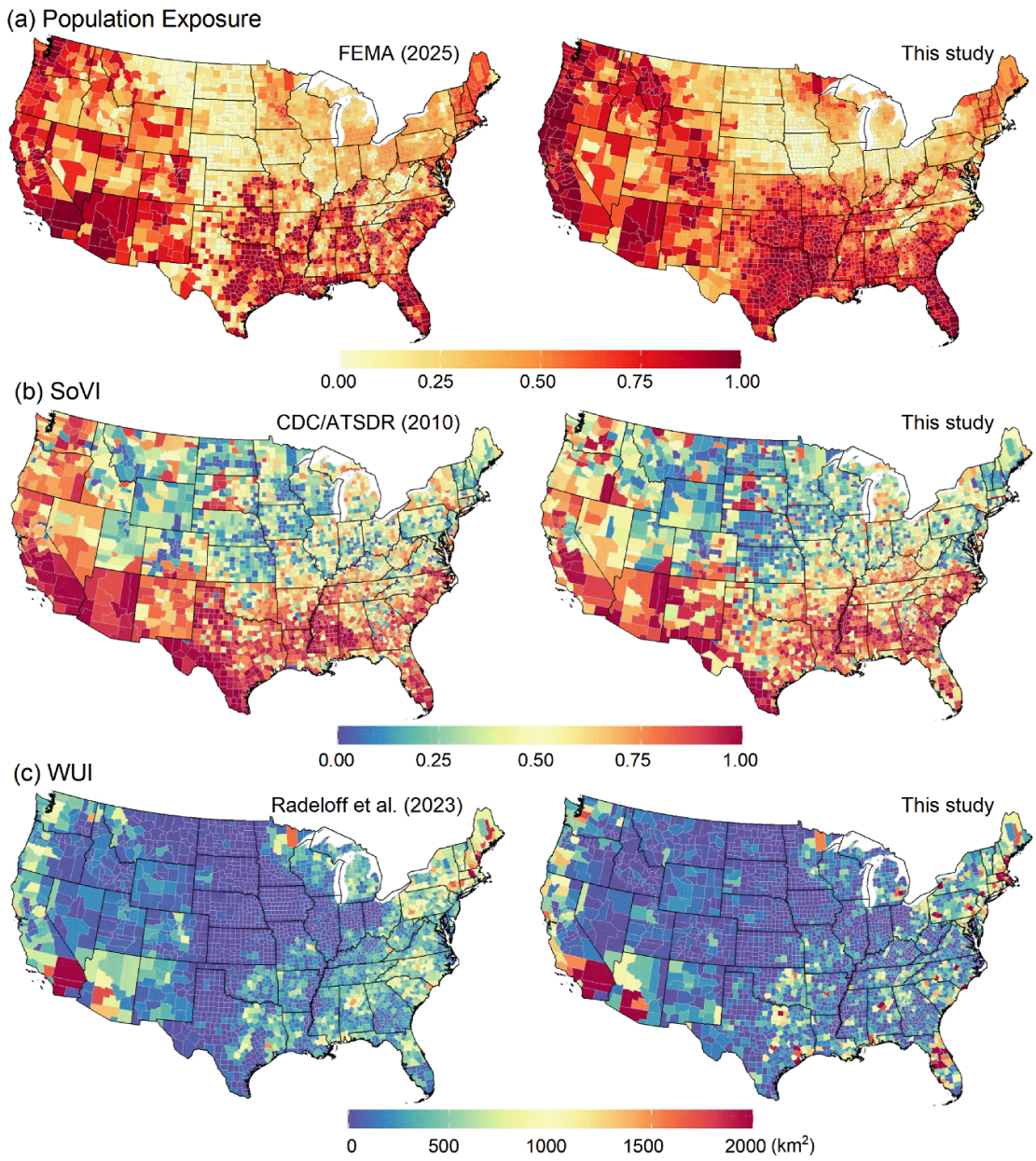


Figure 2. Comparison of historical wildfire population exposure (a), social vulnerability index (SoVI; b), and wildland-urban interface (WUI) area (c) between previous studies and this study. Wildfire population exposure is compared with Federal Emergency Management Agency [FEMA] (2025), whose estimates represent conditions in 2021, whereas our estimates are averaged over 2005–2014. All exposure estimates between Federal Emergency Management Agency [FEMA] (2025) and our study are normalized to a 0–1 scale using national percentile ranks due to differences in units. SoVI from CDC/ATSDR (2010) and this study were similarly normalized for comparison, with higher SoVI values indicating greater social vulnerability. CDC/ATSDR (2010) derives SoVI from 14 social indicators at the US Census tract level, while our study uses 5 county-level indicators (equation (2). For WUI, our approach applies a simplified calculation based on gridded wildland and urban fractions (equation (3) for the year 2015, whereas Radeloff *et al* (2023) identify the intermix and interface WUI patterns from housing and land cover data at the US Census block level for the year 2010.

the Southeast and Northeast (figure 2(c)), whereas the low WUI areas occur in the agriculturally dominated Great Plains, in a good agreement with Radeloff *et al* (2023; $r = 0.78$; $p < 0.001$). However, our estimates tend to identify larger WUI extent in metropolitan counties and their surroundings, including Los Angeles and San Diego (California), Phoenix (Arizona), Houston (Texas), Orlando (Florida); Philadelphia and Pittsburgh (Pennsylvania), and Boston (Massachusetts).

Total wildfire risk (combining both population and property factors) exhibits a heterogeneous spatial pattern during the historical period (figure 3(a)). Counties with the greatest risk, particularly in western mountains, the Rocky Mountain region, and the southern temperate forests, tend to have larger BAs, greater composition of WUI, and higher social vulnerability (i.e. Clusters 1 and 2 in figure 3(b)). In contrast, counties in the Dakotas, Nebraska, Iowa, Illinois, Indiana, and Ohio are generally classified as

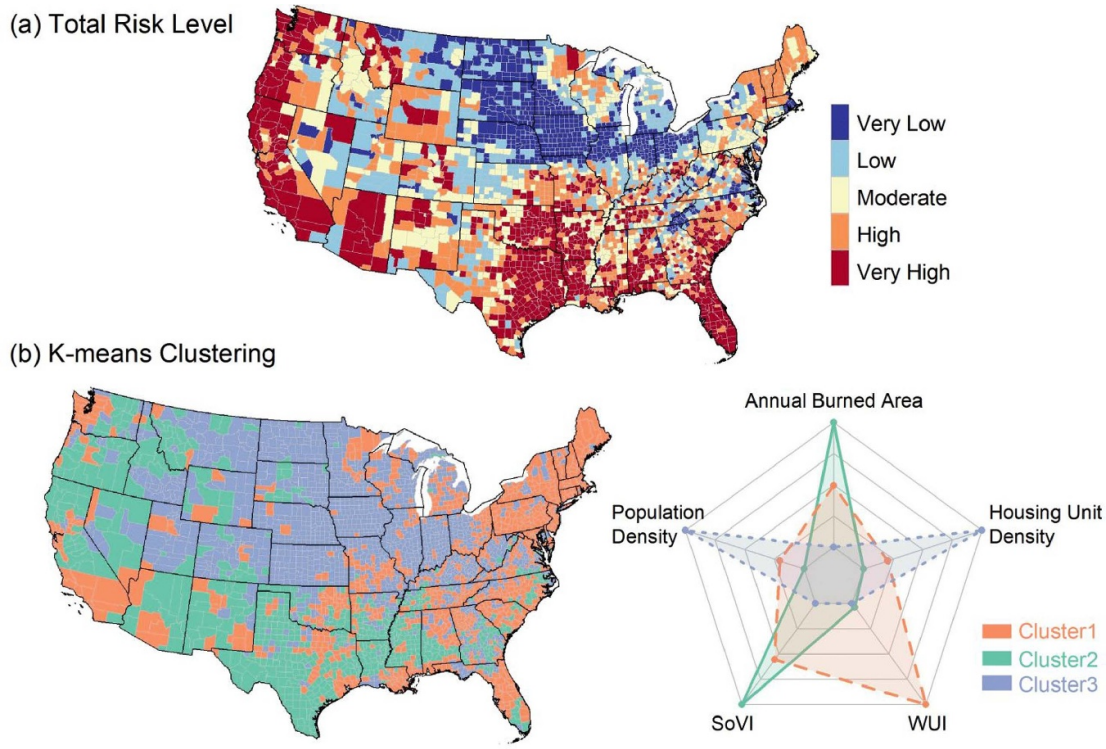


Figure 3. Total wildfire risk levels (population and property) and *K*-means clustering results for the historical baseline period (2005–2014). *K*-means clustering identified three distinct county groups characterized by different combinations of wildfire exposure, social vulnerability, and human development patterns (see text S1 in the supplementary information for details of the clustering method). In the radar plot (bottom right), greater extension along an axis indicates a higher contribution of the corresponding variable to that cluster.

Low or Very Low risk according to our results, owing to sparse WUI, low SoVI, and small annual BAs (figure 3(b)). Meanwhile, the majority of shrubland-dominated counties in southern Idaho, Utah, and Colorado also contribute a considerable amount of fire activity, but they remain identified as Moderate or lower risk in our study because of their low SoVI and limited WUI area (figure 3(b)).

3.2. Future trends in wildfire risk

Compared with the historical baseline, population changes (+9%–46% mid term; −12% to +125% long term; see figure 4(a); figure S2 in the supplementary information), together with expansions in wildfire BA (+18%–49% and +29%–103% for the same periods; see figure 4(b); figure S1 in the supplementary information), are expected to drive substantial growth in future population exposure. Median exposure across all counties is projected to increase by 22%, 58%, and 125% in the mid term, and by 31%, 37%, and 261% in the long term under SSP1-26, SSP3-70, and SSP5-85, respectively (figure 5(a)). When further combined with increases in SoVI (figure 4(c)), these factors translate into population risk scores rising by 27%–162% in the mid term and 54%–411% in the long term for the three pathways (figure 5(b)).

A similar magnitude of change is observed for property exposure (figure 5(c)); however, its risk score increases (7%–72% mid term; 19%–160% long term; median values across all counties under the three SSPs) are smaller than those of population risk (figure 5(d)). This difference likely reflects the temporal-spatial dynamics in WUI contraction over the future periods. Specifically, total WUI areas across the CONUS are projected to decline by 9%–19% by the end of the century (figure 4(d) and figures S6–S7 in the supplementary information), leading to decreased housing risk in states such as Wisconsin, Illinois, Indiana, and Michigan, where future wildfire distribution is expected to remain similar to the historical baseline. Conversely, western regions—including California, Arizona, and Texas—experience substantial growth in BA, but reduced WUI extent would mitigate building exposure, resulting in wildfire risk that is only slightly higher, or even lower in some counties, than historical levels (figure 4(d)).

Under all three future SSPs, the geographic spread of total wildfire risk—integrating population and property components—largely mirrors the historical pattern, with distinct hotspots in the western and southern regions and low-risk areas across the northern Great Plains (figure 6(a)). Notably, states such as the Dakotas, Nebraska, Iowa, Illinois, and Indiana, which have historically been considered low-risk

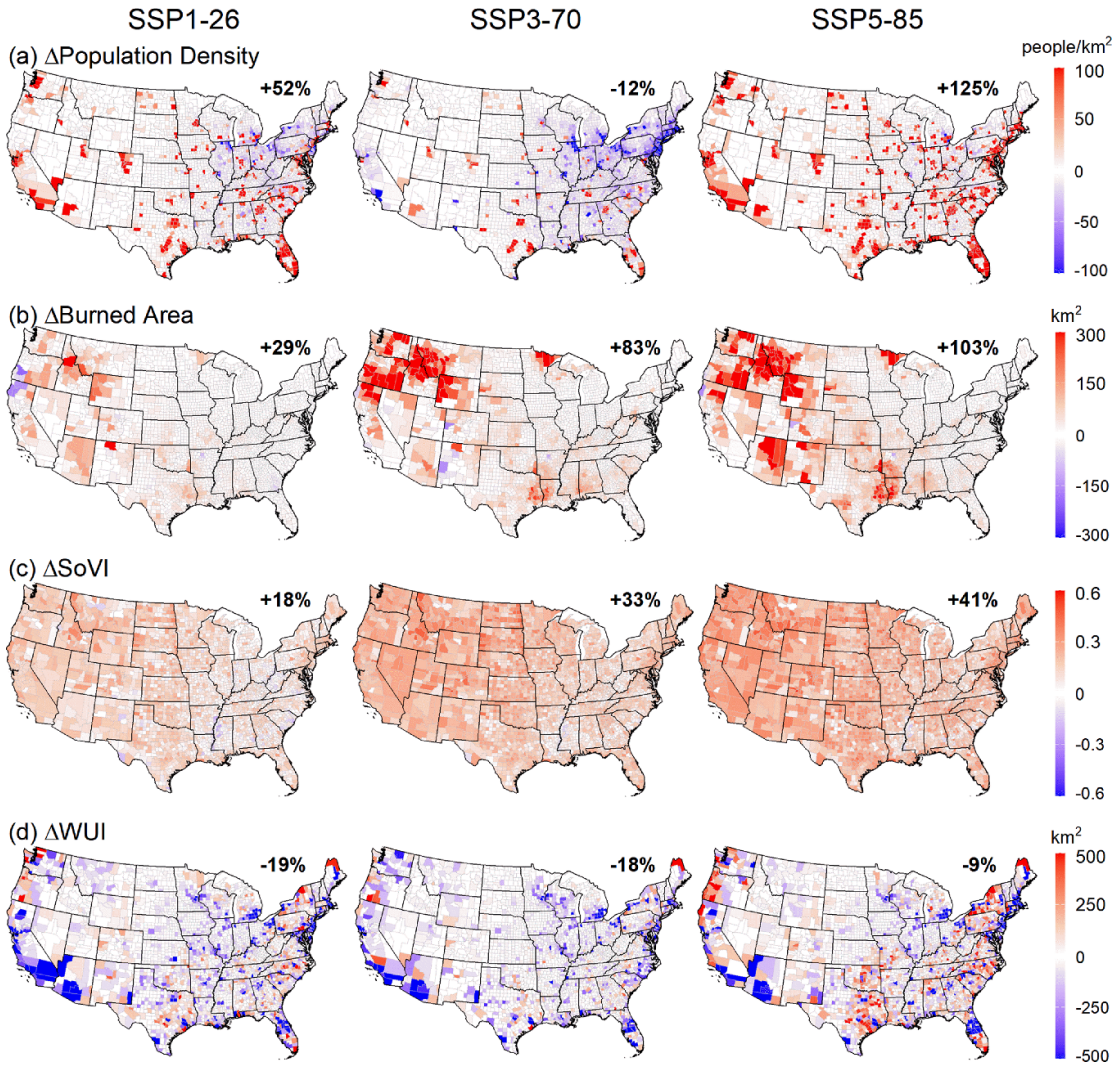


Figure 4. Absolute changes in population density (a), burned area (b), social vulnerability index (SoVI) (c), and wildland-urban interface (WUI) (d) under three future SSP scenarios for the late 21st century (2091–2100), compared with the historical baseline period (2005–2014). The value shown in each panel indicates the 10-year mean relative change (%) over the CONUS for 2091–2100 relative to 2005–2014.

areas, exhibit upward risk transitions across all three scenarios. The numbers of counties transitioning from very low risk to low or moderate risk levels increase progressively from SSP1-26 to SSP3-70 and SSP5-85 (figure 6(b)), primarily associated with increased social vulnerability and population exposure (figure S8 in the supplementary information). In contrast, changes in property risk appear to play a limited role in these transitions (figure S9 in the supplementary information), as both WUI extent and BA show relatively modest changes in these regions under future scenarios (see figure 4).

4. Discussion and Conclusion

This study provides a comprehensive national-scale assessment that jointly quantifies future population and property wildfire risks under multiple SSP scenarios by integrating wildfire hazard, exposure, social vulnerability, and the WUI. Beyond mapping future risk, our analysis reveals county-level transitions in wildfire risk categories, providing insights into how and where wildfire risk may intensify. Our findings indicate that future wildfire risk is projected to increase across many parts of the United States, driven by demographic and settlement shifts, rising social vulnerability, and greater fire probability. Although the magnitude of both population and property risks increases progressively from SSP1-26 to SSP3-70 and SSP5-85 (figure 5), the relative spatial distribution of wildfire risk remains broadly consistent (figure 6). Historically high-risk regions continue to experience elevated wildfire risk, indicating that existing wildfire risk hotspots are likely to persist throughout the century. Therefore, future wildfire risk

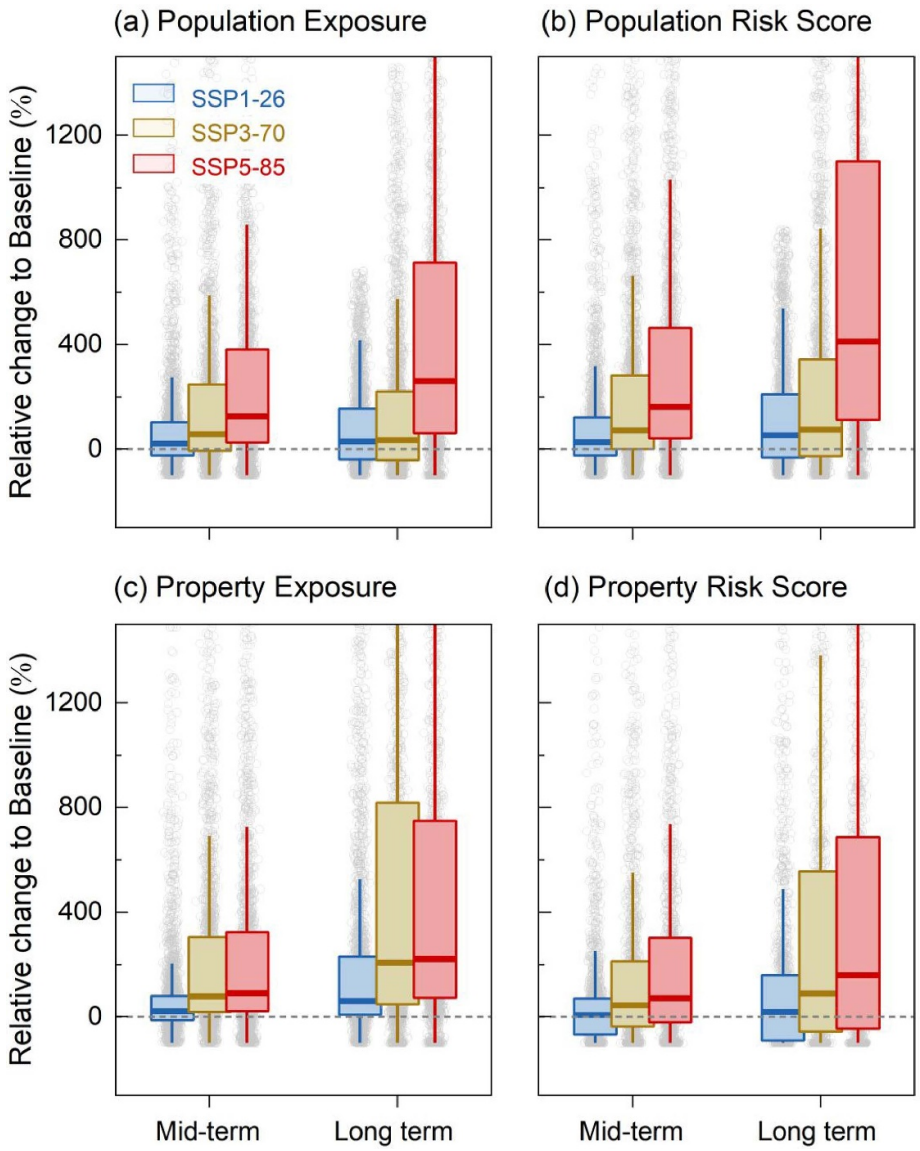


Figure 5. Relative changes (%) in population and property exposure and risk score under three future SSP scenarios for the mid-term (2041–2050) and long term (2091–2100), compared to the historical baseline period (2005–2014). Box plots show the median and interquartile range (IQR) across all 3109 U.S. counties (denoted as gray open circles). Whiskers extend to 1.5 times the IQR from the first and third quartiles. The box edges represent the IQR, and the line inside each box indicates the median.

is characterized more by the intensification of existing risk patterns than by a fundamental redistribution of wildfire risk across the CONUS.

Nevertheless, the observed upward transitions in some historically low-risk regions, particularly across parts of the Midwest, indicate that future wildfire risk is not spatially static. These transitions are primarily associated with increasing population exposure and social vulnerability, whereas changes in property-related risk appear to be comparatively limited. As the U.S. population continues to grow and age, an increasing number of socially vulnerable groups (such as older adults and non-white populations identified in this study) may be exposed to wildfire hazards (figure S4 in the supplementary information), highlighting the critical need to integrate demographic and social vulnerability dimensions into future wildfire planning and mitigation (Rad *et al* 2023a). In addition, although SSP1-26 scenario will be challenging to achieve under current socioeconomic and policy trajectories (O'Neill *et al* 2017, Riahi *et al* 2017), it remains a useful low-emission benchmark for evaluating mitigation benefits. At the other end of the emission spectrum, SSP5-85 is retained as a high-end scenario to explore potential upper-bound wildfire risks, although its underlying emission trajectory is now considered less plausible given recent trends in renewable energy development and climate policies (van Vuuren *et al* 2026). Nevertheless, the projected increase in wildfire risk from SSP1-26 to SSP5-85 in our study highlights the importance of

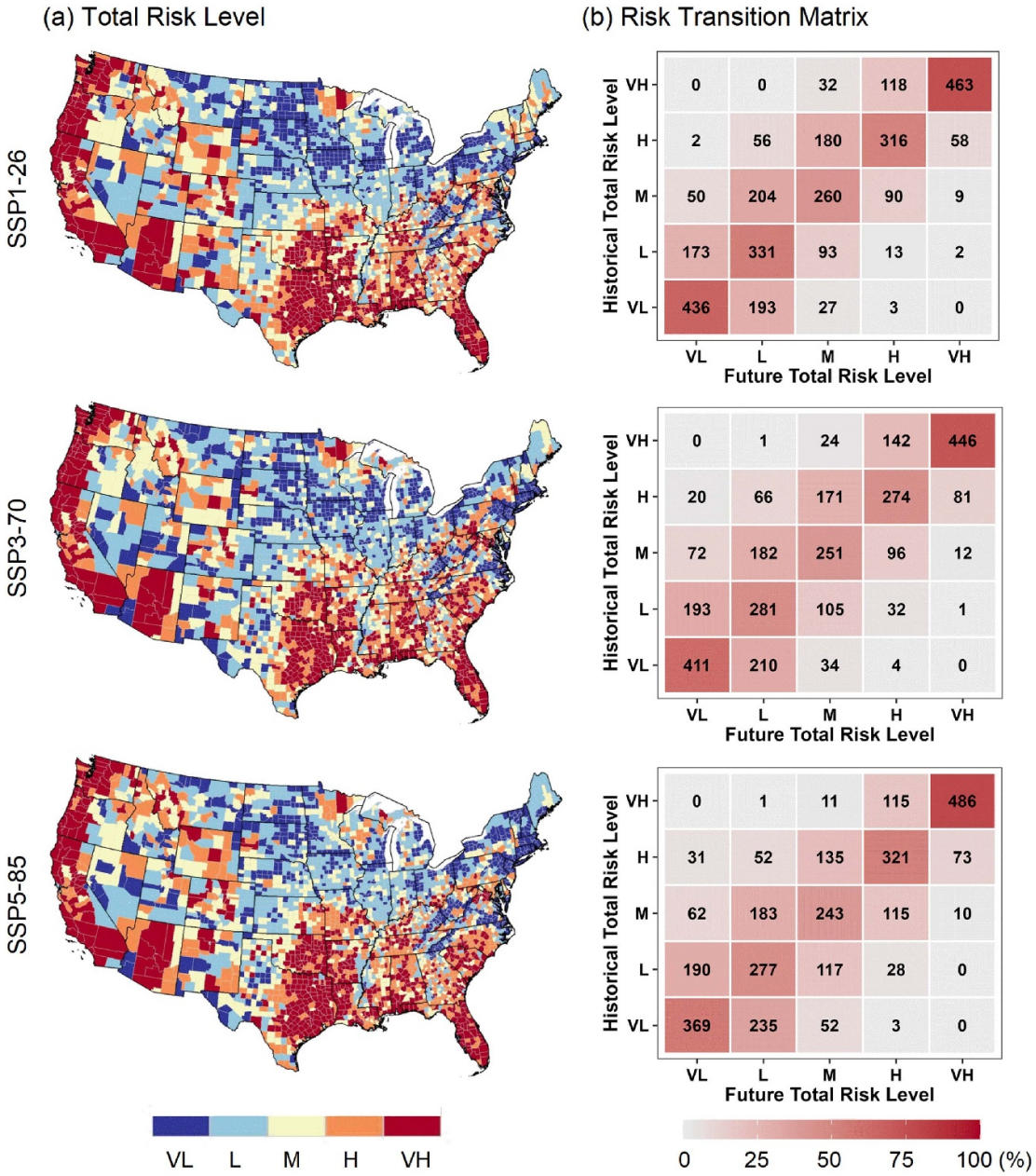


Figure 6. Total wildfire risk levels (population and property risks) under three future SSP scenarios for the long-term period (2091–2100; (a), and their transitions compared with the historical baseline period (2005–2014; (b). The values in (b) represent the number of counties in each transition category, while the colors represent the percentage of counties transitioning from each historical risk level to each future risk level, with each row normalized to sum to 100%. Abbreviation: VL—very low; L—low; M—moderate; H—high; VH—very high.

climate change mitigation, while the persistence of high-risk regions under all scenarios emphasizes additionally the need for continued adaptation.

Our projections represent potential future wildfire risk trajectories under alternative SSP scenarios rather than predictions, with uncertainties arising from future climate pathways, socioeconomic development, and land-use changes. For instance, to evaluate the uncertainty associated with the wildfire hazard component, we compared our BA-based exposure estimates with the recent national assessment by Federal Emergency Management Agency [FEMA] (2025). Some discrepancies persist in parts of the southern counties (figure 2(a)), partly due to overestimated BA from the ELM model used in our analysis (figure S1 in the supplementary information). The overestimation of BA compared with satellite remote sensing is not unique to ELM and has also been reported across all ISIMIP process-based models (Liu *et al* 2025). A likely contributor to the Southeastern bias is the absence of prescribed burning in ELM. These frequent, small fires are widely used in temperate forests of the Southeast to lower fuel loads (Majumder *et al* 2025, Pomara *et al* 2025); their omission leads the model to underrepresent

managed fire activity while overestimating area burned from large wildfires, resulting in net BA overestimation. Another contributing factor might be the use of fixed ignition efficiency to parameterize lightning-caused fires in most process-based models (Rabin *et al* 2017, Liu *et al* 2025), which overlooks the strong spatial variability in lightning frequency and intensity—particularly in the western and southeastern CONUS, where lightning strikes are a key natural ignition source—and may bias BA estimates in this region. In addition, our county-level exposure estimates may introduce uncertainty because BAs and exposed populations are not always spatially aligned within counties, particularly in large counties where fire activity may occur away from populated areas. Future assessments using finer-resolution hazard and exposure datasets could better capture these local-scale spatial relationships.

While this study adopts five indicators—commonly used in other SSP-based assessments (see KC *et al* 2021, Landreau *et al* 2021)—to construct an overall SoVI, it differs from previous studies in how the indicators are weighted and combined. Unlike our equal-weighting approach (equation (2)), Landreau *et al* (2021) applied greater weights to age-related groups and low-income communities based on local expert judgment. Given the projected rapid growth in GDP across the CONUS (figure S4 in the supplementary information), placing more weight on economic capacity could potentially reflect changes in adaptive potential to increasing wildfire-related risks (Paveglio *et al* 2018). However, quantitatively determining such weights remains challenging, due to limited empirical evidence linking future socioeconomic indicators to adaptive capacity. Nevertheless, although our analysis does not include additional variables such as employment, education, and vehicle access—identified as important drivers of wildfire vulnerability in a review by Lambrou *et al* (2023)—our results show good spatial agreement with the SoVI developed by the US Centers for Disease Control and Prevention (CDC/ATSDR 2010), which incorporates 14 demographic and socioeconomic indicators at the census tract level (figure 2(b)). This consistency supports the use of our simplified SoVI framework for scenario-based assessments across current and future periods, while acknowledging that it does not capture all dimensions of social vulnerability.

To approximate future WUI dynamics, we derived wildland and urban fractions from land-use data of Chen *et al* (2022) (equation (3)). The projected changes in WUI therefore reflect changes in the spatial overlap between wildland vegetation and human development under different SSP scenarios, rather than explicit projections of future building locations. While this simplified method captures the broad spatial patterns and magnitude of historical WUI extent across the CONUS, notable discrepancies are found when compared with census block-level statistics (Radeloff *et al* 2023; figure 2(c)). These mismatches partially reflect difference between land-cover-based and building-density-based WUI definitions. In particular, the 0.5%-15% urban land-cover fraction used in our study represents an intermediate level of human development within predominantly wildland landscapes and should not be interpreted as a direct equivalent of the building-density thresholds used in Schug *et al* (2023). Additionally, aggregating the original 1 km land-cover classes to 5 km in our study to calculate wildland and urban fractions may smooth out local heterogeneity (see Text S1 in the supplementary information for details of WUI derivation), leading to overestimation of WUI in metropolitan areas (e.g. Los Angeles, Phoenix, Houston, and Boston), and underestimation in sparsely settled shrubland regions (e.g. Idaho, Nevada, Utah) or densely forested areas with limited urban land (e.g. the Southeast and Northeast). Although future urban-only projections at finer resolutions (see Chen *et al* 2020, He *et al* 2023) could improve WUI estimates, they are not currently harmonized with other land-use components, limiting their integration into a consistent SSP-based framework.

These uncertainties emphasize that our results reflect scenario-based assessments rather than predictions. Nevertheless, the consistent risk patterns and dominant drivers identified here provide useful background for long-term planning. For instance, our study highlights the need for region-specific fire risk mitigation strategies that address the dominant drivers of future wildfire risk. In western and southern CONUS, where wildfire risk remains high due to increasing BA, population density, and social vulnerability, mitigation efforts might continue to prioritize fire suppression and exposure reduction. Although WUI extent is projected to decline in some areas (figure 4), these regions would continue to contain substantial WUI exposure relative to other parts of the country. Therefore, strategies such as fuel management, prescribed burning, and risk-informed WUI planning (Calkin *et al* 2014, Moritz *et al* 2022) remain critical for reducing future wildfire impacts. In contrast, upward risk transitions projected in parts of the Midwest, including the Dakotas, Nebraska, Iowa, and Illinois, are less associated with changes in BA or WUI extent and are more strongly linked to increasing population exposure and social vulnerability. In these regions, mitigation might focus on reducing social vulnerability and enhancing adaptive capacity through emergency preparedness (Yung *et al* 2022), evacuation planning, and community resilience programs (National Fire Protection Association 2017). Under higher-emission

scenarios, such region-specific strategies might become increasingly important as wildfire risk continues to escalate.

Acknowledgment

Famke Geissler and Dr Sam Rabin contributed to the ideas development for this work at a very early stage. Jianyong Ma acknowledges support from the EU EYE-CLIMA project (Grant Agreement No. 101081395).

Data availability statement

The gridded annual burned areas for the historical and future periods estimated by the ELM model are available at: https://data.isimip.org/search/tree/ISIMIP3a/OutputData/fire/ (ISIMIP Repository 2025). Historical county-level population and housing density, along with demographic data, can be downloaded at www.atsdr.cdc.gov/place-health/php/svi/svi-data-documentation-download.html (CDC/ATSDR 2010). Projected county-level population demography under three SSP scenarios can be accessed at https://doi.org/10.17605/osf.io/9ynfc (Hauer 2019). Gridded GDP estimates, state-level Gini coefficient, and gridded land cover data for historical and future periods, are accessible through Zenodo repository at https://zenodo.org/records/7898409 (Wang and Sun 2022), https://zenodo.org/records/7227128 (Casper *et al* 2023), and https://zenodo.org/records/4584775 (Chen *et al* 2022), respectively. This manuscript was polished with the assistance of large language model for text rephrasing and linguistic refinement. All results, interpretations, and scientific content remain solely the responsibility of the authors.

Supplementary material 1 available at https://doi.org/10.1088/2515-7620/aebaf5/data1.

Conflict of interest

The authors declare no conflicts of interest relevant to this study.

Author contributions

Jianyong Ma 0000-0002-9336-5310
Conceptualization (equal), Formal analysis (equal), Methodology (equal), Software (equal), Validation (equal), Visualization (equal), Writing – original draft (equal), Writing – review & editing (equal)

Ashton Dickinson
Formal analysis (equal), Methodology (equal), Software (equal), Visualization (equal), Writing – review & editing (equal)

Anja Rammig
Methodology (equal), Writing – review & editing (equal)

Martin Wittenbrink 0000-0002-6227-7609
Methodology (equal), Writing – review & editing (equal)

Almut Arneth
Conceptualization (equal), Funding acquisition (equal), Writing – review & editing (equal)

References

Ager A A, Day M A, Alcasena F J, Evers C R, Short K C and Grenfell I 2021 Predicting Paradise: modeling future wildfire disasters in the western US *Sci. Total Environ.* **784** 147057

Bar-massada A, Stewart S I, Hammer R B, Mockrin M H and Radeloff V C 2013 Using structure locations as a basis for mapping the wildland urban interface *J. Environ. Manage* **128** 540–7

Begum R A *et al* 2022 Point of Departure and Key Concepts *Climate Change 2022: Impacts, Adaptation and Vulnerability. Contribution of Working Group II to the Sixth Assessment Report of the Intergovernmental Panel on Climate Change* ed H O Pörtner *et al* (Cambridge University Press) pp 121–96

Binita KC, Shepherd J M, King A W and Johnson Gaither C 2021 Multi-hazard climate risk projections for the United States *Nat. Hazards* **105** 1963–76
Bowman D, Williamson G, Abatzoglou J, Kolden C, Cochrane M and Smith A 2017 Human exposure and sensitivity to globally extreme wildfire events *Nat. Ecol. Evol.* **1** 0058
Calkin D E, Cohen J D, Finney M A and Thompson M P 2014 How risk management can prevent future wildfire disasters in the wildland-urban interface *Proc. Natl Acad. Sci. USA* **111** 746–51
Carlson A R, Mockrin M H and Radeloff V C 2022 The wildland-urban interface in the United States based on 125 million building locations *Ecol. Appl.* **32** e2597
Casper K C, Narayan K B, O'Neill B C, Waldhoff S T, Zhang Y and Wejnert-Depue C P 2023 Non-parametric projections of the net-income distribution for all U.S. states for the shared socioeconomic pathways *Environ. Res. Lett.* **18** 114001
CDC/ATSDR 2010 SVI 2010 documentation (available at: www.atsdr.cdc.gov/place-health/php/svi/index.html)
Chen B, Wu S, Jin Y, Song Y, Wu C, Venevsky S, Xu B, Webster C and Gong P 2024 Wildfire risk for global wildland–urban interface areas *Nat. Sustain.* **7** 474–84
Chen G *et al* 2020 Global projections of future urban land expansion under shared socioeconomic pathways *Nat. Commun.* **11** 537
Chen G, Li X and Liu X 2022 Global land projection based on plant functional types with a 1-km resolution under socio-climatic scenarios *Sci. Data* **9** 125
Chuvieco E *et al* 2023 Towards an integrated approach to wildfire risk assessment: when, where, what and how may the landscapes burn *Fire* **6** 215
Cunningham C X, Williamson G J, Bowman D M J S, Cunningham C X, Williamson G J and Bowman D M J S 2024 Increasing frequency and intensity of the most extreme wildfires on Earth *Nat. Ecol. Evol.* **8** 1420–5
Cutter S L, Boruff B J and Shirley W L 2003 Social vulnerability to environmental hazards *Soc. Sci. Q* **84** 242–61
Davies I P, Haugo R D, Robertson J C and Levin P S 2018 The unequal vulnerability of communities of color to wildfire *PLoS One* **13** 1–15
Ellis T M, Bowman D M J S, Jain P, Flannigan M D, Williamson G J, Ellis T M, Bowman D M J S, Jain P, Flannigan M D and Williamson G J 2022 Global increase in wildfire risk due to climate-driven declines in fuel moisture *Glob. Change Biol.* **28** 1544–59
Federal Emergency Management Agency [FEMA] 2025 National risk index technical documentation (available at: www.fema.gov/flood-maps/products-tools/national-risk-index)
Flanagan B E, Gregory E W, Hallisey E J, Heitgerd J L and Lewis B 2011 A social vulnerability index for disaster management *J. Homel. Secur. Emerg. Manage.* **8** 1–22
Flanagan B E, Hallisey E J, Adams E and Lavery A 2018 Measuring community vulnerability to natural and anthropogenic hazards: the centers for disease control and prevention's social vulnerability index *J. Environ. Health* **80** 34–36
Hauer M E 2019 Population projections for U.S. counties by age, sex, and race controlled to shared socioeconomic pathway *Sci. Data* **6** 190005
He W *et al* 2023 Global urban fractional changes at a 1 km resolution throughout 2100 under eight scenarios of shared socioeconomic pathways (SSPs) and representative concentration pathways (RCPs) *Earth Syst. Sci. Data* **15** 3623–39
ISIMIP Repository 2025 [data set] (available at: https://data.isimip.org/search/tree/ISIMIP3a/OutputData/fire/)
Lambrou N, Kolden C, Loukaitou-Sideris A, Anjum E and Acey C 2023 Social drivers of vulnerability to wildfire disasters: a review of the literature *Landsc. Urban Plan* **237** 104797
Landreau A, Juhola S, Jurgilevich A and Räsänen A 2021 Combining socio-economic and climate projections to assess heat risk *Clim. Change* **167** 12
Li F *et al* 2024 Evaluation of global fire simulations in CMIP6 Earth system models *Geosci. Model Dev.* **17** 8751–71
Liu Y, Huang H, Wang S-C, Zhang T, Xu D and Chen Y 2025 ELM2.1-XGBfire1.0: improving wildfire prediction by integrating a machine learning fire model in a land surface model *Geosci. Model Dev.* **18** 4103–17
Majumder R, Terando A J, Hiers J K, Collazo J A and Reich B J 2025 A spatiotemporal optimization engine for prescribed burning in the Southeast US *Ecol. Inform.* **85** 102956
Moritz M A, Hazard R, Johnston K, Mayes M, Mowery M, Oran K, Parkinson A M, Schmidt D A and Wesolowski G 2022 Beyond a focus on fuel reduction in the WUI: the need for regional wildfire mitigation to address multiple risks *Front. For. Glob. Change* **5** 848254
National Fire Protection Association 2017 Firewise USA: residents reducing wildfire risks (available at: www.nfpa.org/education-and-research/wildfire/firewise-usa)
National Interagency Fire Center 2024 Fire-information/statistics (available at: www.nifc.gov/fire-information/statistics)
Nepal S, Pomara L Y, Gould N P and Lee D C 2023 Wildfire risk assessment for strategic forest management in the Southern United States: a Bayesian network modeling approach *Land* **12** 2172
O'Neill B C *et al* 2017 The roads ahead: narratives for shared socioeconomic pathways describing world futures in the 21st century *Glob. Environ. Change* **42** 169–80
O'Neill B C, Kriegler E, Riahi K, Ebi K L, Hallegatte S, Carter T R, Mathur R and van Vuuren D P 2014 A new scenario framework for climate change research: the concept of shared socioeconomic pathways *Clim. Change* **122** 387–400
Paveglio T B, Edgeley C M and Stasiewicz A M 2018 Assessing influences on social vulnerability to wildfire using surveys, spatial data and wildfire simulations *J. Environ. Manage* **213** 425–39
Pomara L Y, Gould N P, Nepal S, Emmett K D, Goodrick S L and Lee D C 2025 Fire: an analysis to support the southern forest outlook (available at: https://research.fs.usda.gov/treesearch/69155)
Rabin S S *et al* 2017 The fire modeling intercomparison project (FireMIP), phase 1: experimental and analytical protocols with detailed model descriptions *Geosci. Model Dev.* **10** 1175–97
Rad A M *et al* 2023a Social vulnerability of the people exposed to wildfires in U.S. West Coast states *Sci. Adv.* **9** eadh4615
Rad A M, Abatzoglou J T, Kreitler J, Alizadeh M R, AghaKouchak A, Hudyma N, Nauslar N J and Sadegh M 2023b Human and infrastructure exposure to large wildfires in the United States *Nat. Sustain.* **6** 1343–51
Radeloff V C *et al* 2018 Rapid growth of the US wildland-urban interface raises wildfire risk *Proc. Natl Acad. Sci. USA* **115** 3314–9
Radeloff V C, Hammer R B, Stewart S I, Fried J S, Holcomb S S and McKeefry J F 2005 The wildland-urban interface in the United States *Ecol. Appl.* **15** 799–805
Radeloff V C, Mockrin M H, Helmers D, Carlson A, Hawbaker T J, Martinuzzi S, Schug F, Alexandre P M, Kramer H A and Pidgeon A M 2023 Rising wildfire risk to houses in the United States, especially in grasslands and shrublands *Science* **382** 702–7
Riahi K *et al* 2017 The Shared Socioeconomic Pathways and their energy, land use, and greenhouse gas emissions implications: an overview *Glob. Environ. Change* **42** 153–68

Schug F *et al* 2023 The global wildland–urban interface *Nature* **621** 94–99
Seydi S T, Abatzoglou J T, Jones M W, Kolden C A, Filippelli G, Hurteau M D, Aghakouchak A, Luce C H, Miao C and Sadegh M 2025 Increasing global human exposure to wildland fires despite declining burned area *Science* **389** 826–9
Turco M, Abatzoglou J T, Herrera S, Zhuang Y, Jerez S, Lucas D D, AghaKouchak A and Cvijanovic I 2023 Anthropogenic climate change impacts exacerbate summer forest fires in California *Proc. Natl Acad. Sci.* **120** e2213815120
van Vuuren D P *et al* 2026 The scenario model intercomparison project for CMIP7 (ScenarioMIP-CMIP7) *Geosci. Model Dev.* **19** 2627–56
Wang T and Sun F 2022 Global gridded GDP data set consistent with the shared socioeconomic pathways *Sci. Data* **9** 221
Wigtil G, Hammer R B, Kline J D, Mockrin M H, Stewart S I, Roper D and Radeloff V C 2016 Places where wildfire potential and social vulnerability coincide in the coterminous United States *Int. J. Wildl. Fire* **25** 896–908
Wu C, Venevsky S, Sitch S, Mercado L M, Huntingford C and Staver A C 2021 Historical and future global burned area with changing climate and human demography *One Earth* **4** 517–30
Yung L, Gray B J, Wyborn C, Miller B A, Williams D R and Essen M 2022 New types of investments needed to address barriers to scaling up wildfire risk mitigation *Fire Ecol.* **18** 30
Zhang G, Wang M, Yang B and Liu K 2024 Current and future patterns of global wildfire based on deep neural networks *Earth's Futur.* **12** e2023EF004088
Zuzak C, Mowrer M, Goodenough E, Burns J, Ranalli N and Rozelle J 2022 The national risk index: establishing a nationwide baseline for natural hazard risk in the US *Nat. Hazards* **114** 2331–55